Reactions of Laser-Ablated Vanadium Atoms with Dioxygen. Infrared Spectra of VO, VO_2, $OOVO_2$, and V_2O_2 in Solid Argon

George V. Chertihin, William D. Bare, and Lester Andrews*

Department of Chemistry, University of Virginia, Charlottesville, Virginia 22904-1000

Received: February 13, 1997; In Final Form: April 16, 1997[⊗]

Laser-ablated V atoms react with O_2 to give primarily the bent VO_2 dioxide molecule and a smaller yield of the monoxide VO. The OVO valence angle is estimated as 118 ± 3° from oxygen isotopic ν_3 frequencies and 121° from DFT calculations. New absorptions appear on annealing to 35 K that can be assigned to two V_2O_2 isomers and the superoxo adduct to VO_2, namely the $OOVO_2$ molecule. Both VO_2 and $OOVO_2$ reveal weak $\nu_1 + \nu_3$ combination bands, which support the assignment of ν_1 and ν_3 fundamental vibrations.

Introduction

Vanadium oxides are of considerable chemical interest due to their wide range of applications as semiconductors, optical devices, catalysts, and coatings.[1−5] Although solid vanadium oxides have been thoroughly studied, little is known about the reaction products of vanadium and dioxygen in the gas phase. Chemiluminescence from VO has been observed,[6] kinetics of V atom reactions with O_2 have been studied,[7] and dissociation energies of VO and VO_2 have been determined from effusion−mass spectrometric experiments.[8] The VO molecule has been studied extensively,[9−13] in part because it is important in the spectra of stars,[12,13] and VO has been identified by ESR spectroscopy in solid matrices.[14,15] The VO_2 molecule has been the subject of two matrix investigations,[15,16] and the $OOVO_2$ species has been suggested from $V(CO)_6$ photolysis with excess dioxygen.[17] The structure of VO_2 is of interest for comparison with other transition metal dioxides important in high-temperature chemistry such as TiO_2, CrO_2, and FeO_2.[18−20]

Experimental Section

The technique for laser ablation and FTIR matrix investigation has been described previously.[18−20] Vanadium metal (Alfa, 99.5%) was mounted on a rotating (1 rpm) stainless steel rod. The Nd:YAG laser fundamental (1064 nm, 10 Hz repetition rate, 10 ns pulse width 40−50 mJ pulses) was focused on the target through a hole in the CsI cryogenic (10 K) window. Metal atoms were codeposited with 0.25−1% O_2 ($^{16}O_2$,$^{18}O_2$, $^{16,18}O_2$, and mixtures) in argon at 2−4 mmol/h for 1−3 h periods. FTIR spectra were recorded with 0.5 or 0.125 cm^{-1} resolution on a Nicolet 750. Matrix samples were temperature cycled, and more spectra were collected; selected samples were subjected to broad-band photolysis with a medium-pressure mercury arc (Philips, 175 W) with globe removed (240−580 nm) at different stages in the annealing cycles.

Results

Infrared spectra of the laser-ablated V + O_2 reaction system will be presented. Spectra are shown in Figure 1, and absorption bands are listed in Table 1 for argon matrix experiments. Deposition with low laser power and low oxygen concentration produced the major band at 935.9 cm^{-1}, although other weak bands were also observed. Increasing oxygen concentration enhanced intensities of all bands. Annealing behavior revealed

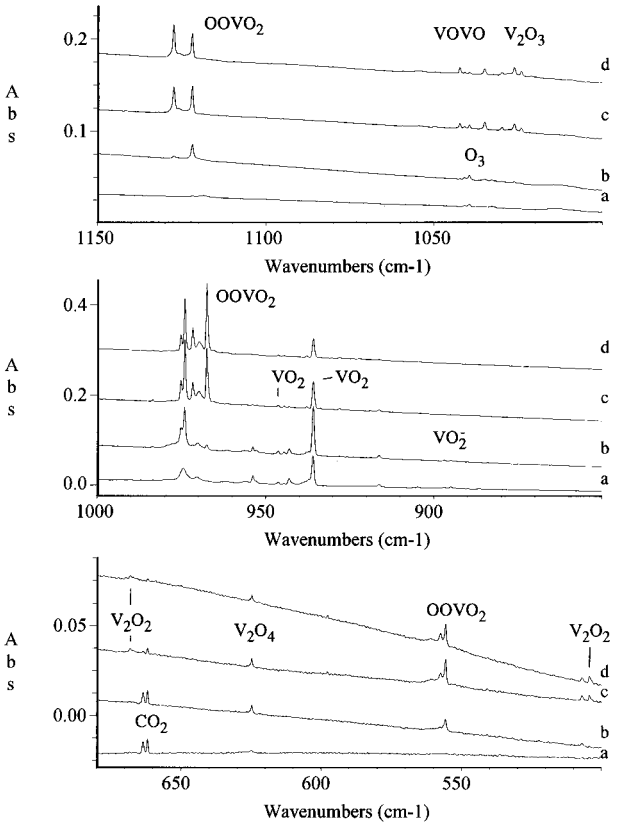

Figure 1. Infrared spectra of sample prepared by reacting laser-ablated V atoms with 0.5% O_2 in argon: (a) 2 h codeposit on 10 ± 1 K window, (b) after annealing to 25 ± 1 K, (c) after annealing to 35 ± 1 K, and (d) after annealing to 40 ± 1 K.

a correlation between 1121.9, 974.1, 555.6 cm^{-1} (site a) and 1127.2, 967.5, 557.4 cm^{-1} (site b) bands, which grew significantly on annealing. The 946.3 and 935.9 cm^{-1} bands grew 50% on annealing to 25 K (Figure 1b) and decreased on further annealing. The 1042.4 and 1026.2 cm^{-1} bands appeared in the spectra only after annealing and increased with different rates (Figure 1c,d); the latter band was relatively more intense with higher oxygen concentration, and the site a bands were favored over the site b bands at higher (1%) O_2 concentration. The latter bands and the 1127.2, 1121.9 cm^{-1} band groups decreased on broad-band photolysis performed after 35 K annealing. The weak 983.6 cm^{-1} band appeared in the spectra after deposition and increased on annealing to 25 K and decreased at higher temperature. The 983.6, 946.3, and 935.9 cm^{-1} bands doubled

[⊗] Abstract published in *Advance ACS Abstracts,* June 15, 1997.

S1089-5639(97)00559-8 CCC: $14.00

TABLE 1: Infrared Absorptions (cm^{-1}) Observed for $V+O_2$ Reaction Products in Solid Argon

$^{16}O_2$	$^{18}O_2$	$^{16}O_2 + {}^{16}O^{18}O + {}^{18}O_2$	$R(^{16}O/^{18}O)$	anneal[b]	assignment
1939.0	1859.5	1938.4, 1859.8	1.0428	+ +	$OOVO_2$ site a ("$\nu_1 + \nu_3$")
1929.4	1850.1		1.0429	+ +	$OOVO_2$ site b ("$\nu_1 + \nu_3$")
1873.0	1794.0	1873.0, 1830.1, 1794.0	1.0440	+ −	OVO ($\nu_1 + \nu_3$)
1871.1	1792.0		1.0441	+ −	OVO site
1127.2	1061.7	*1127.2*, 1096.2, 1094.4, (*1070.3*), *1061.7*[a]	1.0617	+ +	$OOVO_2$ site b
1121.9	1055.3	*1121.9*, 1091.1, 1088.6, (*1064.7*), *1055.3*[a]	1.0629	+ +	$OOVO_2$ site a
1042.4	1000.3	1042.2, 1032, 1031, 1000.4	1.0421	+	VOVO
1026.2	983.5	1034.9, 1025.4, 988.8, 984.3	1.0434	+	OVOVO
1024.2	981.5	1023.7, 981.8	1.0435	+	OVOVO site
983.6	941.1	983.6, 941.1	1.0452	+ −	VO
975.3	932.0	975.3, 932.0	1.0466	+ +	$OOVO_2$ site a ("ν_1")
974.1	936.7	974.1, 936.7	1.0399	+ +	$OOVO_2$ site a ("ν_3")
971.9	934.7	971.9, 934.7	1.0398	+	$(O_2)VO_2$ ("ν_3)
970.2	933.4	970.2, 933.4	1.0394	+	$(O_2)VO_2$ ("ν_3")
967.6	930.5	967.6, 930.5	1.0399	+ +	$OOVO_2$ site b ("ν_3")
953.8	917.5		1.0396	−	OVO−X site
946.3	902.1	946.3, 940.1, 902.1	1.0490	+ −	OVO (ν_1)
943.0	906.3		1.0405	−	OVO site (ν_3)
935.9	899.9	935.9, (900.2), 899.9	1.0400	+ −	OVO (ν_3)
928.0	891.9	928.1, 891.9	1.0406	+	OVO site (ν_3)
896.9	862.9	896.9, 862.9	1.0394	−	VO_2^-
894.3	861.1	894.3	1.0386	−	VO_2^-
801 br	767	800, 791, 788, 768	1.044	+	V_xO_y?
804.2 w	759.0		1.0596	−	O_3^-
752.6	721.7	752.5, 738.8, 721.8	1.0428	+ −	V_2O_4
746.9 w	716.3	746.9, 730.2, 716.3	1.0428	+	?
720.3 w	691.5		1.0416	+ −	?
668.1	640.1	668.1, 652.2, 640.1	1.0437	+	V_2O_2
624.8	595.9	624.5, 611.7, 596.4	1.0485	+ −	V_2O_4
597.7 w	570.0		1.0486	+	V_2O_3
557.4	537.0		1.0380	+	$OOVO_2$ site b
555.6	533.4	*555.6*, 554.4, *553.5*, 552.3, 533.3, 538.2, *536.3*, 534.9, *533.4*[a]	1.0416	+ +	$OOVO_2$ site a
506.9	483.0	*506.9*, *504.2*, 502.3, 500.2, 488.7, *486.5*, 484.7, *483.0*[a]	1.0495	+	$(O_2)VO_2$
504.3	481.9		1.0465	+	V_2O_2

[a] Italic bands observed with $^{16}O_2 + {}^{18}O_2$ mechanical mixture. [b] The + and − refer to increase and decrease of band absorbances on annealing.

on photolysis immediately after deposition, but photolysis after annealing to 35 K decreased the 983.6 cm^{-1} band and increased the 946.3 and 935.9 cm^{-1} bands by 30%. The 896.6/894.3 cm^{-1} doublet appeared after deposition with high laser power and was stronger when the 946.3 and 935.9 cm^{-1} bands were stronger and was destroyed by photolysis or annealing. Finally, the 624.9 cm^{-1} band was observed after deposition and increased on annealing up to 25 K and decreased thereafter.

Oxygen isotopic substitution was employed for band identification. Band positions for the $^{18}O_2$ reaction are also given in Table 1. Experiments were also done with mechanical ($^{16}O_2 + {}^{18}O_2$) and statistical ($^{16}O_2 + {}^{16}O^{18}O + {}^{18}O_2$) mixtures. Figures 2−5 compare isotopic spectra in important regions.

Generally, relative intensities of bands did not depend much on oxygen concentration. In order to change the oxidant, experiments with N_2O were done. All product bands were weaker, but the relative yield of the 983.6 cm^{-1} band is higher than 935.9 cm^{-1} band, the bands around 970 cm^{-1} were very weak even after annealing, and no bands were observed above 1000 cm^{-1} or below 600 cm^{-1}. Absorptions in the 937−950 cm^{-1} region and a 916.3 cm^{-1} band were enhanced as compared with oxygen experiments.

Similar experiments were also done with O_2 in excess nitrogen. Strong bands were observed in the 1800−2300 cm^{-1} region for dinitrogen complexes and at 997.0 cm^{-1} for the VN molecule.[21] Of most interest here, nitrogen matrix counterparts of the major bands were observed. The strongest band on deposition at 942.7 cm^{-1} decreased on annealing, which also produced marked growth in weak bands at 1126.4, 968.8, and 561.8 cm^{-1}. Photolysis yielded a new 944.7 cm^{-1} satellite of double the absorbance. The upper band became a doublet (1126.4, 1060.8 cm^{-1}) and the lower band a quartet (561.8, 559.4, 541.5, 539.3 cm^{-1}) with the mechanical mixture and the upper band a quartet (1126.4, 1195.4, 1093.0, 1060.7 cm^{-1}) and the lower band a higher multiplet (561.8, 560.4, 559.4, 558, 543.1, 541.7, 540.5, 539.3 cm^{-1}) with the statistical mixture whereas the middle band gave only pure isotopic components (968.8, 933.1 cm^{-1} and satellites) with both mixtures. The 942.7, 944.7 cm^{-1} bands gave 907.2, 909.0 cm^{-1} $^{18}O_2$ counterparts and the sum of pure isotopic components with both mixtures. Although the region 1045−980 cm^{-1} was complicated by O_3 and VN absorptions, weak bands that appeared at 1029.0, 1027.0 cm^{-1} could be counterparts of the 1026.2, 1024.2 cm^{-1} argon matrix bands; this could not be confirmed by isotopic substitution.

Discussion

The vanadium oxide molecules produced here will be assigned in turn, and reaction mechanisms will be discussed.

VO. The 983.6 cm^{-1} band was observed after deposition and increased slightly on annealing up to 25 K and decreased on annealing to higher temperatures. The oxygen-18 counterpart at 941.1 cm^{-1} gave the 16/18 isotopic ratio (1.0452), which is just below the harmonic diatomic value (1.0453) as expected. Unfortunately, overlapping of bands with isotopic mixtures prevented the observation of these bands. This band must be considered for the vanadium monoxide molecule based on the gas phase fundamental[9] at 1001.5 cm^{-1}.

First, the 983.6 cm^{-1} band is red-shifted 17.9 cm^{-1} from the gas phase VO fundamental; this compares favorably with TiO, which is red-shifted 12.2 cm^{-1} by the solid argon matrix.[18] Second, this assignment is in good agreement with previous theoretical calculations (1028 cm^{-1}).[22] The present DFT/B3LYP calculations with 6-311+G* basis sets for both V and O atoms, using the Gaussian 94 program[23] found a quartet VO

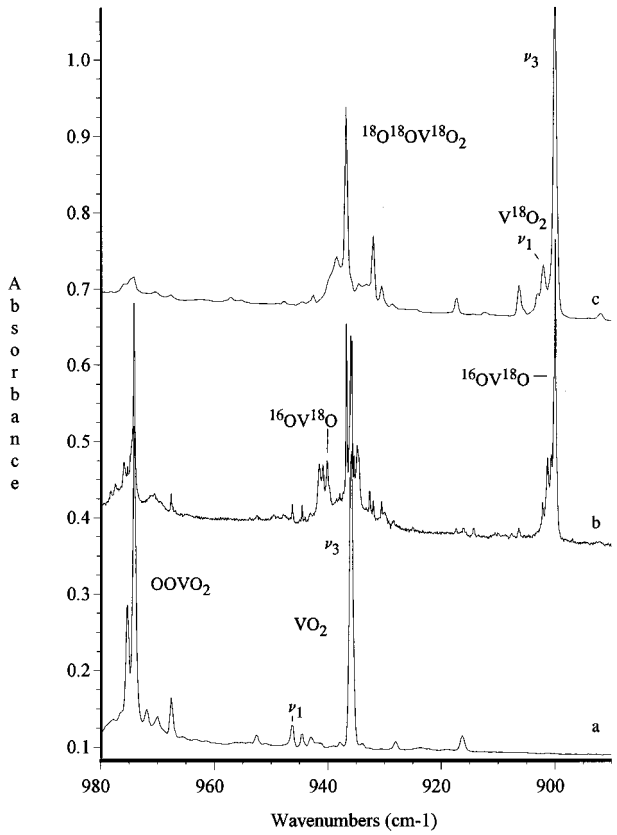

Figure 2. Infrared spectra in the 980−890 cm^{-1} region for major V + O_2 reaction products in solid argon after annealing to 25 K: (a) $^{16}O_2$, 1%, 0.5 cm^{-1} resolution; (b) ($^{16}O_2$ + $^{16}O^{18}O$ + $^{18}O_2$), 0.25%, 0.125 cm^{-1} resolution; (c) $^{18}O_2$, 0.5%, 0.5 cm^{-1} resolution.

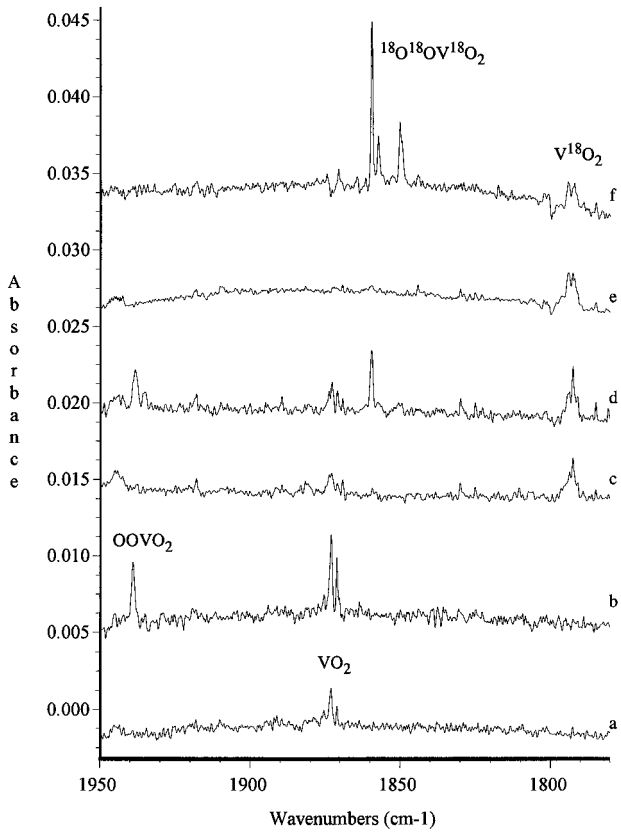

Figure 3. Infrared spectra in the 1950−1780 cm^{-1} region for major V + O_2 reaction products in solid argon: (a) $^{16}O_2$, 1%, deposition; (b) after 25 K anneal; (c) ($^{16}O_2$ + $^{16}O^{18}O$ + $^{18}O_2$), 0.5%, deposition; (d) after 30 K anneal; (e) $^{18}O_2$, 0.5%, deposition; (f) after 35 K anneal.

ground state with a 952 cm^{-1} fundamental, which is lower than experimentally observed. Hence, the 983.6 cm^{-1} band is assigned to VO in solid argon.

Previous work on the V + H_2O argon matrix system reported bands at 1029.7 and 987.2 cm^{-1} after deposition which grew on photolysis.[24] Both bands produced ^{18}O shifts but no deuterium shifts. The first band was assigned to the VO molecule by comparison with the gas phase value,[9] although the 16/18 isotopic ratio (1.0439) is significantly lower than the harmonic diatomic value. The second band was considered to be a "slightly perturbed" version of VO. However, the 42.5 cm^{-1} shift seems too large for a slight perturbation. Moreover, the 1026.2 and 983.6 cm^{-1} bands observed here are just 3.5 cm^{-1} below the band positions reported earlier, which could be due to calibration (grating instrument used previously).[24] Thus, the bands from the V + H_2O system and the present bands are probably due to the same products. The upper band, as it will be shown below, is due to the VOVO molecule, which explains why the isotopic ratios in the previous and present experiments are different from the diatomic value.

VO_2. The present spectra revealed sharp weak 946.3 cm^{-1} and strong 935.9 cm^{-1} bands after deposition, which grew together on photolysis and on annealing to 25 K. The weak features at 953.6 and 943.0 cm^{-1} are due to less stable matrix sites of the strong 935.9 cm^{-1} band. Isotopic spectra are shown in Figure 2. The 946.3 and 935.9 cm^{-1} bands produced doublets and triplets with mechanical and statistical mixtures with 16/18 ratios of 1.0490 and 1.0400, respectively. These bands are assigned to symmetric and antisymmetric vibrations of the insertion product dioxide OVO. The isotopic ν_3 frequencies give a 121° upper limit to the valence angle, which is in accord with the 111° value calculated for the $^2A_1$ ground state using CASSCF[15] and the 121° value calculated here by B3LYP/DFT, which found a $^2B_1$ ground state. A detailed ESR study showed VO_2 in solid neon to be nonlinear with a $^2A_1$ ground state.[15]

Taking TiO_2 as a model where Ti isotopic ν_3 frequencies predict a 111° lower limit and O isotopic frequencies give a 115° upper limit,[18] in the absence of a second vanadium isotope to determine the valence angle lower limit the VO_2 valence angle can be predicted slightly lower in analogous fashion as 118 ± 3° from the isotopic infrared spectrum. The isotopic triplet structures are very asymmetric and have abnormal intensity distributions due to strong coupling of the $^{16}OV^{18}O$ stretching vibrations; i.e., the two stretching modes of $^{16}OV^{18}O$ are barely resolved from the strong $V^{16}O_2$ and $V^{18}O_2$ bands. The present assignment to OVO requires strong coupling between the two stretching vibrations of $^{16}OV^{18}O$.

DFT/B3LYP calculations with the 6-311+G* basis sets for V and O atoms, using the Gaussian 94 program, were done to support these observations. The ground state of OVO is calculated at this level of theory to be a doublet ($^2B_1$); quartet and doublet V(O_2) and VOO are 79, 106, 106, and 120 kcal/mol higher, respectively. These large energy gaps between the bent dioxide and the cyclic and asymmetric isomers are in accord with the growth of OVO on annealing and the absence of VOO and V(O_2). Most impressive is the match between observed and calculated OVO isotopic frequencies and intensities (Table 2). The observed ν_1 and ν_3 modes are 0.926 ± 0.001 times the calculated values. Furthermore, the "antisymmetric" mode of $^{16}OV^{18}O$ is calculated between ν_1 and ν_3 of $V^{18}O_2$ and unusually weak, while the "symmetric" mode is calculated unusually strong and between ν_1 and ν_3 of $V^{16}O_2$, which is in excellent agreement with the experimentally observed isotopic pattern. According to calculations, the ν_2 vibration of OVO should be below 400 cm^{-1}, and no bands in the 600−400 cm^{-1} region can be assigned to this vibration. The present experi-

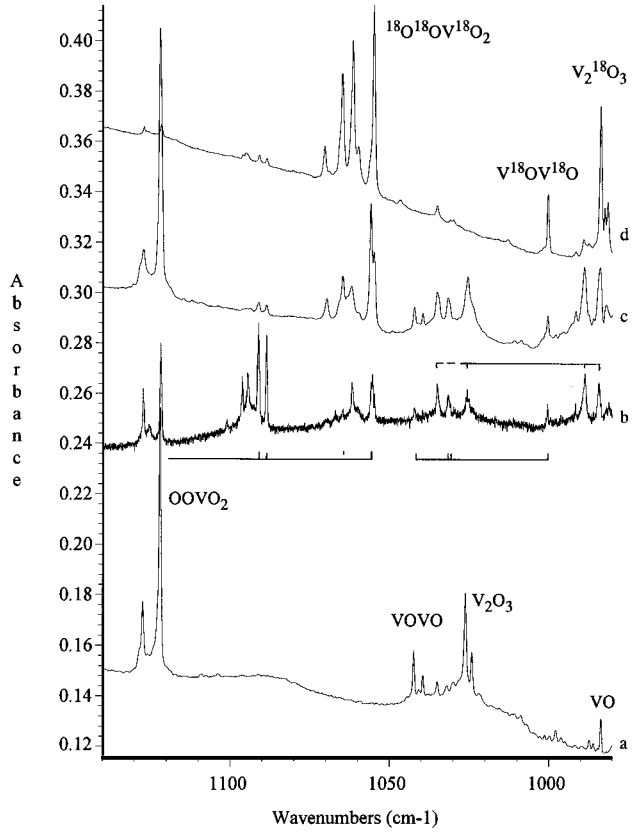

Figure 4. Infrared spectra in the 1140−980 cm^{-1} region after 35 K annealing to maximize product absorptions in this region: (a) $^{16}O_2$, 1%, 0.5 cm^{-1} resolution; (b) ($^{16}O_2$ + $^{16}O^{18}O$ + $^{18}O_2$), 0.25%, 0.125 cm^{-1} resolution; (c) ($^{16}O_2$ + $^{18}O_2$), 1%, 0.5 cm^{-1} resolution; (d) $^{18}O_2$, 0.5%, 0.5 cm^{-1} resolution.

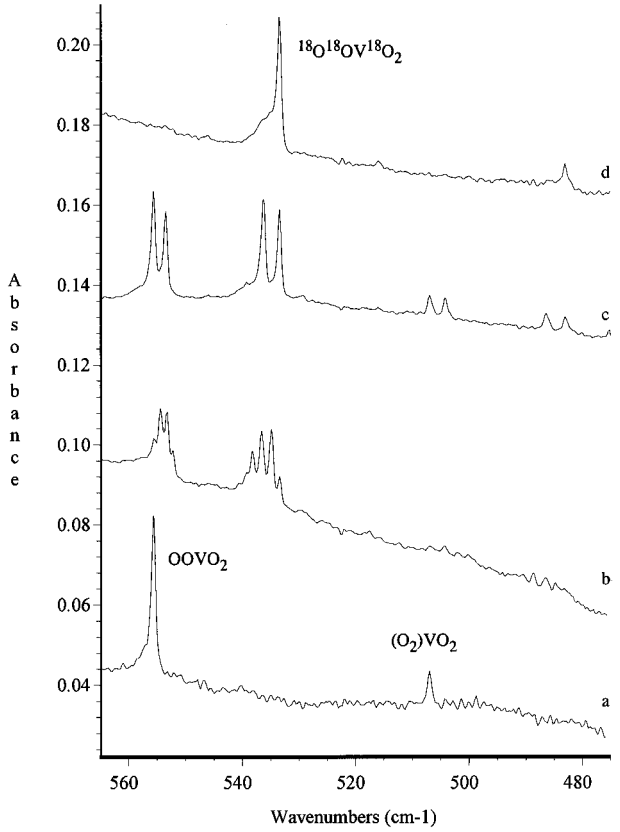

Figure 5. Infrared spectra in the 570−470 cm^{-1} region after 35 K annealing to maximize product absorptions in this region: (a) $^{16}O_2$, 1%; (b) ($^{16}O_2$ + $^{16}O^{18}O$ + $^{18}O_2$), 0.5%; (c) ($^{16}O_2$ + $^{18}O_2$), 1%; (d) $^{18}O_2$, 0.5%.

mental and theoretical results clearly show that the previous VO_2 vibrational assignments are incorrect.[16]

For the analogous bent OCrO molecule, very strong ν_3 and weaker ν_1 modes were observed at 965.4 and 914.4 cm^{-1}, respectively, and their combination gave a very weak band at 1869.7 cm^{-1}. In the $^{16}OCr^{18}O$ case mode mixing gave slightly asymmetric mixed isotopic triplet fundamental bands, and the combination band gave a 1:2:1 triplet.[19] Figure 3 shows the VO_2 combination band region. The sum of ν_1 (a_1) and ν_3 (b_1) fundamentals for $^{16}OV^{16}O$ (946.3 + 935.6 = 1881.9 cm^{-1}) and for $^{18}OV^{18}O$ (902.1 + 899.9 = 1802.0 cm^{-1}) are 8.9 and 8.0 cm^{-1}, respectively, higher than the sharp, weak combination bands observed at 1873.0 and 1794.0 cm^{-1}. The sum of strongly interacting stretching fundamentals for $^{16}OV^{18}O$ (940.1 + 900.2 = 1840.3 cm^{-1}) is 10.2 cm^{-1} higher than the weaker band observed at 1830.1 cm^{-1}. Anharmonic coupling is different in the $V^{16}O_2$ and $V^{18}O_2$ (C_{2v}) and $^{16}OV^{18}O$ (C_s) molecules, and even though the population of $^{16}OV^{18}O$ is about double that of $V^{16}O_2$ or $V^{18}O_2$, its combination band is weaker. Nevertheless, observation of the $\nu_1 + \nu_3$ combination band for VO_2 isotopic molecules confirms the present fundamental vibrational assignments.

A 916.3 cm^{-1} band grew after annealing and produced doublets with isotopic mixtures. This band was enhanced in experiments with N_2O, and it is tentatively be assigned to nitrogen perturbed VO_2, i.e., $(N_2)_xVO_2$.

VO_2^-. The doublet at 896.9/894.3 cm^{-1} was observed after deposition and disappeared after annealing. Isotopic substitution with mechanical and statistical mixtures revealed isotopic doublets in both cases with 16/18 ratio of 1.0394, which is just slightly lower than that for ν_3 of OVO. The deposition and annealing behaviors do not associate this doublet with any vanadium−oxygen complex, and the negative ion OVO^- is proposed. The isotopic ratio suggests that the anion has a slightly more open angle (125°) than the neutral molecule. A similar situation was found[18] for TiO_2 and TiO_2^-. Very asymmetric isotopic structure due to mode coupling was observed for VO_2, and probably this is also the case for OVO^-, which is confirmed by calculations.

DFT calculations found $^3A_1$ and $^1A_1$ anions; the singlet is ruled out because it is higher by 14 kcal/mol and is more bent and has symmetric and antisymmetric vibrations with almost the same intensities, and clear triplet isotopic structures should be observed for each vibration. In contrast, the antisymmetric vibration of the triplet anion is more intense than the symmetric one, and this anion has a slightly more open angle (Table 2). Furthermore, only a doublet absorption should be observed on isotopic substitution, because one stretching vibration of $^{16}OV^{18}O^-$ is very close to the asymmetric mode of $V^{16}O_2^-$. Again, the stability and formation of the negative ion can be rationalized by increasing of electron affinity from monoxide to dioxide molecules, which is observed for several transition metals.[25] These results also agree with the recent observation of VO_2^- in mass spectra.[26]

Bent VOVO. The 1042.4 cm^{-1} band appeared in the spectra recorded after annealing. It produced a quartet isotopic structure with both mechanical and statistical mixtures, and the 16/18 isotopic ratio 1.0421 is lower than the diatomic value. The quartet isotopic structure suggests two inequivalent oxygen atoms, and this band is assigned to the VOVO molecule. The mode is primarily antisymmetric −O−V−O as characterized by the isotopic ratio.

V_2O_2 Ring. In like fashion a 668.1 cm^{-1} band was produced on annealing to 25 K and increased on further annealing cycles. The band produced a clear triplet at 668.1, 652.2, 640.1 cm^{-1} with both mechanical and statistical isotopic mixtures and a 16/18 ratio 1.0437, which is below the diatomic value, but still

TABLE 2: Calculated Structure, Vibrational Frequencies (cm^{-1}), and Intensities (km/mol) for VO_2 Isomers and VO_2^- Anion Using B3LYP/DFT

molecule	structure (Å, deg)	ν_1 (*I*)	ν_2 (*I*)	ν_3 (*I*)
$^{16}OV^{16}O$ doublet	R(VO) = 1.612 α = 121	1023 (44)	311 (16)	1010 (493)
$^{16}OV^{18}O$		1016 (230)	304 (15)	972 (289)
$^{18}OV^{18}O$		974 (41)	297 (14)	972 (458)
V(O_2) doublet	R(V−O) = 1.815 α = 48	869 (240)	626 (94)	489 (11)
quartet	R(V−O) = 1.817 α = 46	942 (213)	629 (21)	409 (13)
VOO doublet	R(V−O) = 1.732 R(O−O) = 1.279 α = 180	1260 (672)	464 (44)	144 (4)
quartet	R(V−O) = 1.708 R(O−O) = 1.288 α = 180	1207 (905)	554 (2)	183 (16)
$^{16}OV^{16}O^-$ singlet	R(V−O) = 1.619 α = 110	994 (300)	360 (8)	975 (275)
$^{16}OV^{18}O^-$		986 (291)	351 (8)	942 (255)
$^{18}OV^{18}O^-$		950 (291)	343 (8)	936 (249)
OVO^- triplet	R(V−O) = 1.655 α = 124	921 (149)	284 (0.1)	923 (409)
$^{16}OV^{18}O^-$		882 (231)	278 (0.1)	922 (300)
$^{18}OV^{18}O^-$		877 (132)	272 (0.1)	888 (373)

characteristic of a V−O vibration. A weaker 504.3 cm^{-1} tracked on annealing shifted to 481.9 cm^{-1} on $^{18}O_2$ substitution and gave a 1.0465 ratio, which is just above the diatomic value. The 668.1 and 504.3 cm^{-1} bands are in the region expected for bridged −V−O− vibrations, and a puckered ring is suggested based on the oxygen isotopic ratios.

V_2O_4. On the other hand, the 624.8 cm^{-1} band is present on deposition, and it grows slightly on annealing to 25 K and then decreases following the behavior of VO_2. The mechanical mixture gives a sharp triplet at 624.8, 611.7, 595.9 cm^{-1} with 16/18 ratio 1.0485, which is near the ratio for the ν_1 mode of VO_2. In contrast, the statistical mixture gives a broader "triplet" at 624.5, 611.7, 596.4 cm^{-1}; note the shifts from pure isotopic band positions. This "triplet" is really an unresolved nonet, which is resolved in the case of the analogous 643.1 cm^{-1} band of Cr_2O_4.[19] The 624.8 cm^{-1} band is tentatively assigned to V_2O_4; the 16/18 ratio suggests an antisymmetric combination of symmetric V−O_2 stretching modes. A weaker 752.6 cm^{-1} band is associated on annealing and photolysis (slight increase and formation of blue-shifted shoulder). This band also exhibits weak triplets with both isotopic mixtures and a 16/18 ratio (1.0428) characteristic of an antisymmetric V−O_2 stretching motion.

OVOVO. The site-split doublet 1026.2/1024.2 cm^{-1} appeared in the spectra after annealing. The yield of this product was enhanced in experiments with higher oxygen concentration. Isotopic substitution produced complicated structures. The ^{16}O and ^{18}O doublets 1026.2/1024.2 and 983.5/981.4 cm^{-1} were always sharper and narrower in experiments with $^{16}O_2$/Ar and $^{18}O_2$/Ar than in experiments with mechanical and statistical mixtures. Moreover, both mixtures gave broadened bands at 1034.9, 1025.4, 988.8, and 984.3 cm^{-1}. (Annealing to 25 K showed that the 1034.9 cm^{-1} band is associated with the 1026.2 and not the 1042.4 cm^{-1} band.) Assuming coupling between stretching vibrations in isotopically mixed molecules, the whole isotopic structure is an unresolved asymmetric sextet coupled with the 1034.9 cm^{-1} band. The 16/18 isotopic ratio 1.0434 differs from both VO and VO_2 ratios. Based on these results a "w-shaped" OVOVO molecule is the leading candidate for the assignment. The weak 597.7 cm^{-1} band in the low-frequency region behaved very similarly on annealing; unfortunately, due to band weakness only the ^{18}O counterpart was detected. The 16/18 oxygen isotopic ratio 1.0486 is appropriate for a symmetric vibration of the V−O−V fragment of a nonlinear V_2O_3 molecule. An analogous picture was observed earlier for the Ti_2O_3 molecule, whose two upper and lower bands showed oxygen isotopic ratios higher and lower than the diatomic ratio, respectively.[18]

Note that observation of both VOVO and OVOVO molecules is in good agreement with the recent results obtained for the Co, Ni, and Cu + O_2 systems obtained in this laboratory. For the later transition metals, both MOMO and OMOMO molecules were found in the higher frequency region.[27−29] The direct combination of OVO and VO is the most favorable mechanism for OVOVO formation on annealing in these experiments. This band was probably observed in the V + H_2O system, which was mentioned earlier. For the V_2O_3 identification suggested here to be correct, V_2O_3 would have to evaporate from the thermal vanadium source used earlier, as VO was observed (our reassignment), but not VO_2, in the V + H_2O experiment.[24]

$OOVO_2$. The three major bands, namely, 1121.9, 974.1, and 555.6 cm^{-1}, were observed after annealing to 25 K. Further annealing led to growth of the weaker 1127.2, 967.5, and 557.4 cm^{-1} bands and weak additional features at 971.9 and 970.2 cm^{-1}. In each group the 974.1 and 967.5 cm^{-1} bands were the most intense, respectively. The $^{18}O_2$/Ar experiments revealed an unusual picture in the upper region: the 1061.7 and 1055.3 cm^{-1} bands (^{18}O counterparts of the 1127.2 and 1121.9 cm^{-1} bands) were always accompanied by extra bands at 1070.3, 1064.7 cm^{-1}. The 16/18 isotopic ratios for the first group of bands were 1.0629, 1.0399, and 1.0416, while for the second group 1.0617, 1.0399, and 1.0380, respectively. Experiments with mechanical isotopic mixture found doublet, doublet, and quartet absorption patterns for both groups. Again, the 1070.3, 1064.7 cm^{-1} bands were observed. Scrambled oxygen experiments revealed quartet and doublet and at least octet isotopic structures, respectively, for both groups. Based on these results, the product contains two inequivalent dioxygen subunits, and the $OOVO_2$ molecule is proposed from the O−O and antisymmetric VO_2 stretching nature of the major vibrations. In addition, a slightly different band profile in $^{16}O_2$ and $^{18}O_2$ experiments shows that the weaker 975.3 cm^{-1} satellite has a lower 932.0 cm^{-1} isotopic counterpart and is the corresponding symmetric VO_2 stretching mode. The present experiments found that bands from both groups grew in the same proportion on annealing; bands from the second group were not observed without bands from the first group, and the second group bands were less intense than those from the first group. In other words,

TABLE 3: Calculated Structure, Highest Vibrational Frequencies (cm^{-1}), and Intensities (km/mol) for Isotopic $OOVO_2$ Molecules[a]

$^{16}O^{16}OV^{16}O_2$	1269 (46)[b]	1071 (261)[c]	1062 (244)[d]	542 (25)[e]	338 (9)[f]	253 (38)[f]
1616−1618	1269 (48)	1071 (261)	1018 (226)	539 (26)	332 (8)	253 (38)
1616−1818	1269 (51)	1028 (278)	1016 (190)	536 (24)	324 (8)	252 (36)
1816−1616	1239 (40)	1071 (267)	1067 (238)	534 (24)	336 (9)	251 (39)
1618−1616	1230 (41)	1071 (267)	1062 (242)	533 (22)	336 (9)	244 (37)
1818−1616	1199 (29)	1070 (278)	1061 (234)	526 (22)	334 (10)	242 (38)
1816−1618	1239 (38)	1071 (264)	1017 (225)	532 (24)	330 (9)	251 (39)
1618−1618	1230 (44)	1071 (264)	1018 (226)	530 (22)	329 (9)	245 (36)
1818−1618	1198 (32)	1070 (268)	1017 (226)	524 (22)	327 (9)	242 (38)
1816−1818	1238 (42)	1028 (281)	1016 (188)	529 (24)	322 (8)	250 (37)
1618−1818	1229 (48)	1028 (280)	1016 (191)	527 (22)	322 (9)	244 (35)
1818−1818	1197 (38)	1027 (284)	1016 (189)	521 (22)	320 (9)	241 (36)

[a] Structure: the superoxo O−O length is 1.277 Å, the O−VO_2 length is 1.84 Å, the V−O_2 lengths are 1.586 Å, and the included angle is 112° and the O−O−V angle is 152°; the O−O species is approximately in the plane bisecting the VO_2 angle. [b] Terminal O−O stretching mode. [c] Antisymmetric V−O_2 stretching mode. [d] Symmetric V−O_2 stretching mode. [e] Antisymmetric OO−V−O_2 stretching mode. [f] Mixed bending modes O−O−V and O−V−O.

the $OOVO_2$ molecule has at least two matrix sites (or orientations of the superoxo ligand) and the first and the second group of bands belong to the two major sites, while weak features at 971.9 and at 506.9 cm^{-1} are due to minor sites. Note that only one site absorbing at 1126.4, 968.8, and 561.8 cm^{-1} was observed for $OOVO_2$ in solid nitrogen; these bands exhibited similar isotopic shifts in nitrogen and argon matrices. Finally, note that the 16/18 ratio for $OOVO_2$ (1.0399) is virtually unchanged from the VO_2 value, showing that binding of a superoxo ligand to VO_2 does not change the VO_2 angle (±1°)! Note that for the OVO molecule highly asymmetric isotopic structures were observed with scrambled oxygen due to strong coupling between stretching vibrations of the isotopically mixed molecule. This coupling exists for the VO_2 subunit in the case of $OOVO_2$, which leads to the observation of "doublets". The low-frequency bands from each group are connected with a metal vibration; roughly speaking it is an antisymmetric motion of V between oxygen subunits (OO−V−O_2). A slight structural difference between these $OOVO_2$ species is suggested by the slightly different 16/18 ratios for the low-frequency modes.

Of further interest are the isotopic ratios of the upper bands and observation of an additional band for the oxygen-18 isotopic molecule. This region is characteristic of the O−O vibration, but this mode should have a 16/18 ratio equal to or less than the harmonic diatomic oxygen ratio of 1.0607. Moreover, the 1127.2 and 1121.9 cm^{-1} matrix site bands have slightly higher but not equal isotopic ratios (1.0629 and 1.0617). Fermi resonance between the overtone of the low-frequency vibration and the O−O vibration is the strongest for the ^{18}O isotopomer of $OOVO_2$ in a matrix site, and it leads to red-shifting of the $^{18}O-^{18}O$ fundamental, further increasing the isotopic ratio, and observation of a new band at 1064.7 cm^{-1} in $^{18}O_2$ experiments. In other words the 1064.7 and 1055.3 cm^{-1} bands are a Fermi doublet; note that the center of gravity is (1064.7 + 1055.3)/2 = 1060.0 cm^{-1} and that the ratio 1121.9/1060.0 = 1.0584 is even lower than the diatomic oxygen ratio. Likewise, for the second matrix site the 1070.3 and 1061.7 cm^{-1} bands are a Fermi doublet and 1127.2 divided by the 1066.0 mean (1.0574) is lower still.

Finally, these vibrational assignments find confirmation in observation of a weak combination band for the "ν_3" and "ν_1" modes of the VO_2 submolecule in $OOVO_2$ as was also found for isolated VO_2. The sums of fundamentals for $OOV^{16}O_2$ (975.3 + 974.1 = 1949.4 cm^{-1}) and for $OOV^{18}O_2$ (932.0 + 936.7 = 1868.7 cm^{-1}) are respectively 10.4 and 9.2 cm^{-1} higher than the observed combination bands at 1939.0 and 1859.5 cm^{-1} for the first site. The second site revealed corresponding combination bands at 1929.4 and 1850.1 cm^{-1} for the $OOV^{16}O_2$ and $OOV^{18}O_2$ molecules. An intermediate combination band was not found for $OOV(^{16}O^{18}O)$.

The assumption that the $OOVO_2$ molecule has at least two sites in the matrix can be also confirmed by the following. Almond and Atkins[9] assigned 1129.0, 969.5, 960.0, and 563.5 cm^{-1} bands to this molecule, which was produced by photooxidation of $V(CO)_6$ in the presence of oxygen. Note that the positions of their bands differ slightly, which cannot be explained by calibration (Perkin-Elmer 983 with 0.5 cm^{-1} resolution was used in the previous work), because upper and lower bands are higher while middle bands are lower than the present observations. The most probable explanation is that they observed not $OOVO_2$ but its complex with CO or the presence of CO changes the matrix structure and distribution of possible sites. The lower frequency mode at 506.9 cm^{-1} exhibits the same VO_4 stoichiometry but a higher 16/18 ratio. It is presumed that this molecule has a slightly different structure than sites a and b of $OOVO_2$. The 971.9 and 970.2 cm^{-1} bands that grow on annealing are clearly due to antisymmetric V−O_2 stretching motions, and annealing behavior is consistent with their association with the 506.9 cm^{-1} absorption. However, no other bands can be associated with this species. These bands are tentatively assigned to the structural isomer $(O_2)VO_2$, which would have a very weak symmetric (O−O) stretching mode.

The DFT calculations presented in Table 3 showed reverse positions of the symmetric and asymmetric vibrations of the OVO fragment, although these bands are very close (10 cm^{-1} difference). The most impressive are isotopic calculations, which found quartet and doublet isotopic structures for the upper and middle bands. Twelve isotopic bands should be observed for the lower vibration, but since isotopic components are close, only nine bands were resolved.

Higher Vanadium Oxides. The weak bands below 900 cm^{-1} listed in Table 1 are mostly observed after annealing and their isotopic structures were not totally resolved. They are probably due to higher oxides V_xO_y.

Reaction Mechanisms. The reaction of V atoms and O_2 molecules is of interest for comparison with early (Ti) and late (Fe and Ni) transition metal matrix isolation studies[18,20,28,30] and with gas phase reactions.[6,7] The VO molecule is formed directly by reaction 1 during reagent condensation, which is exothermic

$$V + O_2 \rightarrow VO + O \qquad (1)$$

by 28 ± 4 kcal/mol based on bond dissociation energies.[8,9] This reaction proceeds in the gas phase with thermal V atoms[6,7] and probably on annealing to 25 K in solid argon. The small growth of O_3 on annealing from diffusion and reaction of O and O_2 does leave open the possibility that VO is formed by atom combination instead of reaction 1 on annealing.

The observation of strong VO_2 absorption after reagent codeposition indicates that VO_2 is formed directly by reaction 2. In experiments with the $^{16}O_2 + {}^{18}O_2$ mixture, no evidence

$$V + O_2 \rightarrow OVO \tag{2}$$

was found for $^{16}OV^{18}O$ on deposition or on annealing, which increased $^{16}OV^{16}O$ and $^{18}OV^{18}O$ by 10%. This means that reactions 3 do not make a measurable contribution and that

$$O + VO \rightarrow OVO \tag{3a}$$

$$O_2 + VO \rightarrow OVO + O \tag{3b}$$

reaction 2 must be the major route to OVO in these experiments. Although metastable excited V atoms probably contribute to the codeposition reaction, it is apparent from the growth on 25 K annealing that ground state V also inserts into dioxygen. Apparently, no 1:1 complexes between vanadium and oxygen survive as spontaneous reaction to OVO occurs straightaway, since no bands can be associated with possible VOO and $V(O_2)$ product molecules, and the exothermicity of reaction (2), namely, 178 ± 4 kcal/mol, is very high.[8]

Photolysis was done here to separate bands into groups for assignment to specific molecules. Reactions 1 and 2 are probably activated by electronic excitation as broad-band photolysis covering the region of atomic absorptions[7] doubled the VO and OVO absorption intensities.

The major difference between the matrix and gas phase reactions is the presence of many "third body" argon atoms to quench the large exothermicity of the insertion reaction 2 and allow the OVO molecule to be stabilized. Such is the case for Ti and Fe atom reactions, which gave OTiO and OFeO as major products of the matrix codeposition reactions.[18,20]

The lack of observation of a $V(O_2)$ complex parallels matrix work with Ti where no $Ti(O_2)$ complex was found and contrasts Fe and Ni where distinct $Fe(O_2)$ and $Ni(O_2)$ complexes were observed;[18,20,28,30] gas phase studies also found no evidence for a $V(O_2)$ complex intermediate.[7]

Two V_2O_2 isomers were observed; mechanical and statistical isotopic mixtures produced quartet and triplet isotopic structures for the 1042.4, and 668.1 cm^{-1} bands, respectively. This means that the main mechanism for their formation is dimerization of VO, reaction 4, rather than reaction of VO_2 with a second V

$$2VO \rightarrow VOVO \text{ or } V_2O_2 \tag{4}$$

atom. Again, the analogous mechanism was suggested for the formation of the Ti_2O_2, Zr_2O_2, and Hf_2O_2 molecules.[18] This contrasts Fe_2O_2, which was produced from the $FeO_2 + Fe$ reaction.[20] Finally, it is likely that Ti_2O_2 and V_2O_2 are puckered rings whereas Fe_2O_2 and Ni_2O_2 are planar, rhombic rings.[20,28]

Conclusions

Reactions of laser-ablated V atoms and oxygen molecules in a condensing argon stream gave the VO, VO_2, V_2O_2, and $OOVO_2$ molecules, which are identified from oxygen isotopic shifts and splittings and photolysis and annealing behavior. The major primary reaction product VO_2 molecule has a very asymmetric isotopic structure due to strong coupling between stretching vibrations of the isotopically mixed $^{16}OV^{18}O$ molecule. The VO_2 valence angle upper limit (121°) is calculated from the oxygen 16/18 ratio. The VO_2 molecule is also formed in matrices on annealing, which means that this reaction does not require activation energy and explains the absence of other possible isomers of vanadium dioxide. DFT frequency calculations are in excellent agreement with the observed isotopic structure for OVO. The relative calculated stabilities of VO_2 isomers support the conclusion that only the insertion product is formed. The anion VO_2^- is tentatively identified and has a slightly more open angle than the neutral molecule, which is also confirmed by theoretical calculations.

The V_2O_2 molecule is formed by dimerization of VO and exists in two isomeric forms: bent VOVO and cyclic V_2O_2. The presumably "w-shaped" V_2O_3 molecule is produced by reaction of VO_2 and VO. The V_2O_4 molecule appears from dimerization of VO_2.

The most complicated spectra are observed for $OOVO_2$ molecule, which is formed by association of O_2 and VO_2 on annealing. This molecule is characterized by superoxo O−O, $V-O_2$, and $-O-V-O_2$ stretching modes, in reasonable agreement with that prepared from the photolysis of $V(CO)_6$ in the presence of excess O_2.[17]

References and Notes

(1) Wentzcovitch, R. M.; Schultz, W. W.; Allen, P. B. *Phys. Rev. Lett.* **1994**, *72*, 3389 and references therein.
(2) Parker, J. C.; Geiser, U. W.; Lam, D. J.; Xu, Y. N.; Wai, Y. C. *J. Am. Ceram. Soc.* **1990**, *73*, 3206.
(3) Sorantin, P. I.; Schwarz, K. *Inorg. Chem.* **1992**, *31*, 567.
(4) Becker, M. F.; Buckman, B. A.; Walser, R. M.; Leping, T.; Georges, P.; Brun, A. *Appl. Phys. Lett.* **1994**, *65*, 1507.
(5) LeBars, J.; Vedrine, J. C.; Aurous, A.; Pommier, B.; Pajonk, G. M. *J. Phys. Chem.* **1992**, *96*, 2217 and references therein.
(6) Parson, L. M.; Geiger, L. C.; Conway, T. J. *J. Chem. Phys.* **1981**, *75*, 5595.
(7) McClean, R. E.; Pasternack, L. *J. Phys. Chem.* **1992**, *96*, 9828. See also: Ritter, D.; Weisshaar, J. C. *J. Phys. Chem.* **1990**, *94*, 4907.
(8) Farber, M.; Uy, O. M.; Srivastava, R. D. *J. Chem. Phys.* **1972**, *56*, 5312 and references therein.
(9) Huber, K. P.; Herzberg, G. *Constants of Diatomic Molecules*; (Van Nostrand Reinhold: New York, 1979.
(10) Huang, G.; Merer, A. J.; Clouthier, D. J. *J. Mol. Spectrosc.* **1992**, *153*, 32.
(11) Harrington, J.; Weisshaar, J. C. *J. Chem. Phys.* **1992**, *97*, 2809.
(12) Cheung, A. S.-C.; Hajigeorgiou, P. G.; Huang, G.; Huang, S.-Z.; Merer, A. J. *J. Mol. Spectrosc.* **1994**, *163*, 443.
(13) Adam, A. G.; Barnes, M.; Berno, B.; Bower, R. D.; Merer, A. J. *J. Mol. Spectrosc.* **1995**, *170*, 94.
(14) Kasai, P. H. *J. Chem. Phys.* **1968**, *49*, 4979.
(15) Knight, L. B., Jr.; Babb, R.; Ray, M.; Banisaukas, T. J., III; Russon, L.; Dailey, R. S.; Davidson, E. R. *J. Chem. Phys.* **1996**, *105*, 10237.
(16) Serebrennikov, L. V.; Maltsev, A. A. *Vestn. Mosk. Univ., Ser. 2, Khim.* **1980**, *21*, 178.
(17) Almond, H. T.; Atkins, R. W. *J. Chem. Soc., Dalton Trans.* **1994**, 835.
(18) Chertihin, G. V.; Andrews, L. *J. Phys. Chem.* **1995**, *99*, 6356.
(19) Chertihin, G. V.; Bare, W. D.; Andrews, L. *J. Chem. Phys.*, in press.
(20) Chertihin, G. V.; Saffel, W.; Yustein, J. T.; Andrews, L.; Neurock, M.; Ricca, A.; Bauschlicher, C. W., Jr. *J. Phys. Chem.* **1996**, *100*, 5261.
(21) Andrews, L.; Bare, W. D.; Chertihin, G. V. To be published.
(22) Bauschlicher, C. W., Jr.; Maitre, P. *Theor. Chim. Acta* **1995**, *90*, 189.
(23) Gaussian 94, Revision B.1. Frisch, M. J.; Trucks, G. W.; Schlegel, H. B.; Gill, P. M. W.; Johnson, B. G.; Robb, M. A.; Cheeseman, J. R.; Keith, T.; Petersson, G. A.; Montgomery, J. A.; Raghavachari, K.; Al-Laham, M. A.; Zakrzewski, V. G.; Ortiz, J. V.; Foresman, J. B.; Cioslowski, J.; Stefanov, B. B.; Nanayakkara, A.; Challacombe, M.; Peng, C. Y.; Ayala, P. Y.; Chen, W.; Wong, M. W.; Andres, J. L.; Replogle, E. S.; Gomperts, R.; Martin, R. L.; Fox, D. J.; Binkley, J. S.; Defrees, D. J.; Baker, J.; Stewart, J. P.; Head-Gordon, M.; Gonzalez, C.; Pople J. A. Gaussian, Inc., Pittsburgh, PA, 1995.
(24) Kauffman, J. W.; Hauge, R. H.; Margrave, J. L. *J. Phys. Chem.* **1985**, *89*, 3547.
(25) Polak, M. L.; Gilles, M. K.; Ho, J.; Lineberger, W. C. *J. Phys. Chem.* **1991**, *95*, 3460. Hotop, H.; Lineberger, W. C. *J. Phys. Chem. Ref. Data* **1985**, *14*, 731.
(26) Rudnyi, E. B.; Kaibieheva, G. A.; Gidorov, L. N. *J. Chem. Thermodyn.* **1993**, *25*, 929.
(27) Chertihin, G. V.; Citra, A.; Bauschlicher, C. W., Jr. To be published.
(28) Citra, A.; Chertihin, G. V.; Andrews, L.; Neurock, M. *J. Phys. Chem. A* **1997**, *101*, 3109.
(29) Chertihin, G. V.; Andrews, L.; Bauschlicher, C. W., Jr. *J. Phys. Chem. A* **1997**, *101*, 4026.
(30) Huber, H.; Klotzbucher, W.; Ozin, G. A.; Vander Voet, A. *Can. J. Chem.* **1973**, *51*, 2722.